Reprinted from LANGMUIR, 1991, 7.

Modeling the Growth of Semiconductor Epitaxial Films via Nanosecond Time Scale Molecular Dynamics Simulations

Deepak Srivastava and Barbara J. Garrison*

Department of Chemistry, The Pennsylvania State University, University Park, Pennsylvania 16802

Donald W. Brenner

Code 6119, Naval Research Laboratory, Washington, D.C. 20375

Received June 27, 1990

Microscopic and macroscopic growth mechanisms of semiconductor epitaxial films due to Si and Ge deposition on the dimer reconstructed Si{100}-(2 × 1) surface are modeled via molecular dynamics. The forces for solving the classical equations of motion are derived from Tersoff's many-body potential for the multicomponent Si–Ge system. In our model, thermally deposited Si and Ge atoms are allowed to react with the dimer reconstructed Si{100}-(2 × 1) surface for nanosecond durations. For the first time, the *microscopic* mechanisms of the unreconstruction of the original surface and *macroscopic* formation of the epilayers of the deposited material are extracted. We find that the dimer openings on the reconstructed surface following the Si or Ge deposition are either due to a diffusing adatom (the deposited atom) induced mechanism or due to a direct insertion of the incoming adatoms into the epitaxial positions. The results reveal a novel mechanism involving cooperative motion of adatoms in which diffusing adatoms move perpendicular to the direction of the dimer rows of the original surface. The resulting relaxation of the underneath substrate and dimer atoms causes the opening of successive dimers along the way. The mechanism is proposed to be responsible for the kinetics of a dramatic enhancement of the crystal growth process in one direction. This prediction has been recently confirmed by using the scanning tunneling microscope (STM). A total of three to six monolayers of epitaxial Si and Ge have been grown in the simulations. Two distinct layer by layer growth modes of macroscopic epitaxial films are observed. In one case the domains of amorphous regions in the growth remain roughly in the same area of the interface throughout the entire thickness. In the other example the reconstructions on the buried interfaces can be relieved by long time equilibrations. The epitaxially deposited films have a tendency to heal the inner layers during nanosecond time scale equilibrations. In accordance with the Rutherford backscattering experiments we also find that the reconstruction remains at the growing interface.

Introduction

The heteroepitaxial growth of novel semiconductor materials on single-crystal Si substrates is an important economic and technological goal. Efforts on both the theoretical and experimental fronts are being intensely pursued to better understand various microscopic and macroscopic processes associated with the growth of semiconductor thin films. Molecular-beam epitaxy (MBE) is widely employed for semiconductor epitaxial film growth. With this method, atoms or molecules effuse from an oven source of semiconductor material and impinge on a constant temperature semiconductor substrate. The layers of deposited material often form high-quality, defect-free, signal-crystal thin films. Depending upon growth conditions the film could have the same well-defined crystalline structure of the underlying substrate (epitaxial) or it could have a random bonding structures (amorphous). The usual goal is to obtain layer by layer crystalline growth such as alternating bands of two layers of Si and two layers of Ge.[1]

One of the problems with obtaining layer-by-layer growth is the fact that atoms in the surface layer of most semiconductors are significantly displaced from the bulk configuration. Semiconductors such as silicon and germanium tend to crystallize in a bulk diamond form where each atom has four nearest neighbors. The atoms on a freshly cleaned surface, however, do not experience their full coordination, so they tend to react with each other to form a different arrangement (reconstruction) than would be found for the bulk solid. For example, the surface atoms on the bulk terminated Si{100} face (Figure 1a) tend to move closer to the neighboring atoms and form rows of stable dimer structures (Figure 1b). These structures have been confirmed both through theoretical energetics calculations[2] and through direct scanning tunneling microscope (STM)[3,4] studies. These rearrangements do not just constitute the basis of esoteric surface physics experiments. They are extremely important from a microelectronic device point of view. In order for epitaxial growth to occur on a reconstructed surface (Figure 1b), the atoms in the dimerized layer must be reordered back to their original bulk positions, so that the atoms in the deposited layer can be in the expected bulk positions for the next higher layer.

A number of experimental advances now allow one to examine the macroscopic features of thin film growth.[3-5] For example, as mentioned above, the STM takes a "picture" of the surface. The problem from our point of view is that these pictures are taken seconds to minutes (that is, an infinite amount of time) after the interesting chemical reactions of dimer opening or surface rearrangements have occurred. It is in precisely this time domain where computer modeling can play a dominant role in

---

[1] Bevk, J.; Mannaerts, J. P.; Feldman, L. C.; Davidson, B. *Appl. Phys. Lett.* **1986**, *49* (5), 286.

[2] Ihm, J.; Cohen, M. L.; Chadi, D. J. *Phys. Rev. B* **1980** *21*, 4592.

[3] Tromp, R. M.; Hamers, R. J.; Demuth, J. E. *Phys. Rev. Lett.* **1985**, *55*, 1303.

[4] Hamers, R. J.; Tromp, R. M.; Demuth, J. E. *Phys.* Rev. *B* **1986**, *34*, 5343; *Surf. Sci.* **1987**, *181*, 346.

[5] For a recent review, see: Haneman, D. *Rep. Prog. Phys.* **1987**, *50*, 1045.

0743-7463/91/2407-0683$02.50/0

unraveling new scientific principles. Molecular dynamics computer simulations open the door to looking at *microscopic* mechanisms of chemical reactions. In other words, we can watch the motion of the atoms as the chemical reactions are proceeding in the most relevant femtosecond to nanosecond time regime.

Early molecular dynamics simulations[6,7] emphasized growth of epitaxial films that were a few monolayers thick without regard to microscopic processes. In later studies,[8] details of the dimer opening in the initial stages of the epitaxial growth were made. But an extension toward layer by layer growth patterns could not be achieved due to limited computer resources. In this paper we present results of complete molecular dynamics simulations of the epitaxial growth of Si and Ge thin films on the reconstructed Si{100} surface.[9,10] These calculations demonstrate for the first time the utility of large scale molecular dynamics simulations in understanding (i) the atomistic details of individual dimer openings necessary for the initiation of the epitaxial growth, (ii) a collective motion induced spread of dimer openings in the intermediate stages, and (iii) macroscopic modes of growth of epitaxial films that are several layers thick. The computer results reveal a novel mechanism of collective motion of adatoms (deposited atoms) in which the diffusing adatoms move perpendicularly to the dimer rows on the original reconstructed surface and open successive dimers. This mechanism implies that there must be a dramatic enhancement of crystal growth in the direction perpendicular to the direction of dimer rows in the underneath layer.[9] Concurrently with these predictions, the same anisotropy in the early stages of epitaxial growth has also been discovered in STM studies performed by Hamers et al.[11] and Lagally et al.[12] The consequences of these predictions and the observations of an inherently anisotropic growth mechanism during the initial stages of epitaxial growth on the Si{100}-(2 × 1) surface are of major significance. Those systems that exhibit lateral epitaxial growth anisotropy grow with a smaller vertical interface width than systems in which the growth is isotropic.[13,14] Technologically this is a critical point since growth on the (2 × 1) reconstructed {100} face will be smoother than isotropic growth on the other crystal faces.

With our calculations, it is now possible to follow the growth of two to six monolayers of epitaxial Si or Ge films.[10] Two distinct layer by layer growth modes have been discovered. In one case, at low substrate temperature, the growth characteristics of the very initial stages persist during the entire duration of the computer simulations. The initially deposited amorphous region remains amorphous throughout the vertical width of the interface. In the other regime at comparatively higher substrate temperatures, reconstructions at the buried interface are found to be relieved by long-time equilibrations. The epitaxially deposited film exhibits a tendency to heal its inner layers. Consequently, a buried amorphous region can, at a later time, yield high-quality epitaxial growth.

Molecular Dynamics of the Epitaxial Growth Process with Short-Range Many-Body Interaction Potentials

In molecular dynamics simulations of the MBE growth of semiconductor thin films, the gas phase atoms are randomly deposited on a slab of substrate atoms held at a given temperature. The nonequilibrium dynamics of the substrate and the deposited atoms, interacting with realistic many-body forces, is evolved by solving hundreds to thousands of classical equations of motions in finite short time steps ($\sim 10^{-15}$ s) for long time ($\sim 10^{-9}$–10^{-8} s) durations. The correlation between the molecular dynamics simulation growth rates, which then are of the order of one monolayer/ns (1 ns = 10^{-9} s),[9,10] to the typical experimental growth rates, e.g. 0.1 monolayer/min,[15] is achieved by depositing the gas-phase atoms at a much faster rate and equilibrating the whole system for nanosecond durations. It is hoped during these equilibrations that rare event processes such as diffusion and migration take place in an average way and that the growth mechanisms extracted in this way are a realistic representation of the true dynamics. The requirement of integrating hundreds of equations of motion for millions of short time steps has only recently been satisfied by supercomputers. Concurrent with the increase in computational power there has been significant advances in the development of realistic short-range many-body interaction potentials. These potentials accurately describe the chemical behavior of various semiconductor materials.[16-18] For example, Tersoff's many-body interaction potential for the multicomponent Si–Ge system[19] is sufficiently realistic to predict in detail the chemical reaction dynamics of the MBE growth of Si and Ge thin films on the reconstructed Si{100} surface.

Molecular dynamics requires integration of differential equations of the type

$$m\frac{\mathrm{d}^2 r_i}{\mathrm{d}t} = \sum_{j \neq i} f(r_{ij}) \tag{1a}$$

$$f = -\frac{\mathrm{d}E(r_{ij})}{\mathrm{d}r_{ij}} \tag{1b}$$

For each atom i the summation j over the forces $f(r_{ij})$ yields the net force on atom i due to all of the other atoms. For simplicity, in eq 1, we have considered only the pair interactions. In the case of many-body interactions, for each pair of atoms i and j there can be an additional summation k over all the remaining atoms. Numerical integration of these differential equations at each time step requires the gradient of the total energy of the system. This gradient can also be expressed semiempirically as a sum over pair and many-body interaction potentials.[16-19] The interaction potential used in these simulations is Tersoff's many-body potential for Si and Ge.[19] The general form of the potential including the many-body effects in the attractive part is

---

(6) Schneider, M.; Schuller, T. K.; Rahman, A. *Phys. Rev. B* **1987**, *36*, 1340.

(7) Gawlinski, E. T.; Gunton, J. D. *Phys. Rev. B* **1987**, *36*, 4774.

(8) D. W. Brenner and B. J. Garrison, *MRS Symp. Proc.* 1987, *No. 94*, 77; *Surf. Sci.* 1988, *198*, 151.

(9) Srivastava, D.; Garrison, B. J.; Brenner, D. W. *Phys. Rev. Lett.* **1989**, *63*, 302.

(10) Srivastava, D.; Garrison, B. J. *J. Vac. Sci. Technol., A* **1990**, *8*, 3506.

(11) Hamers, R. J.; Köhler, U. K.; Demuth, J. E. *Ultramicroscopy* **1989**, *31*, 10.

(12) Lagally, M. G.; Kariotis, R.; Swartzentruber, B. S.; Mo, Y.-W. *Ultramicroscopy* **1989**, *31*, 87.

(13) Mo, Y.-W.; Kariotis, R.; Sevage, D. E.; Legally, M. G. *Surf. Sci. Lett.* **1989**, *219* L551.

(14) Hamers, R. J.; Köhler, U. K.; Demuth, J. E. *J. Vac. Sci. Technol.* **1990**, *8*, 196.

(15) Gossmann, H.-J.; Feldman, L. C. *Phys. Rev. B* **1985**, *32*, 6.

(16) See, for example, Ackland, G. *Phys. Rev. B* **1989**, *40*, 10351, and references therein for many Si potentials.

(17) Tersoff, J. *Phys. Rev. Lett.* **1989**, *61*, 2879; and Brenner, D. W. *Mater. Res. Soc. Symp. Proc.* **1989**, *141*, 59, for C potentials.

(18) Ding, K.; Andersen, H. C. *Phys. Rev. B* **1987**, *34*, 6987. Grabow, M.; Gilmer, G. H. *Mater. Res. Soc. Symp. Proc.* **1987**, *94*. Ito, T.; Khor, K. E.; Das Sarma, S. *Phys. Rev. B* **1989**, *40*, 9715. Baskes, M. I.; Nelson, J. S.; Wright, A. F. *Phys. Rev. B* **1989**, *40*, 6085, for Ge potentials.

(19) Tersoff, J. *Phys. Rev. B* **1989**, *39*, 5566.

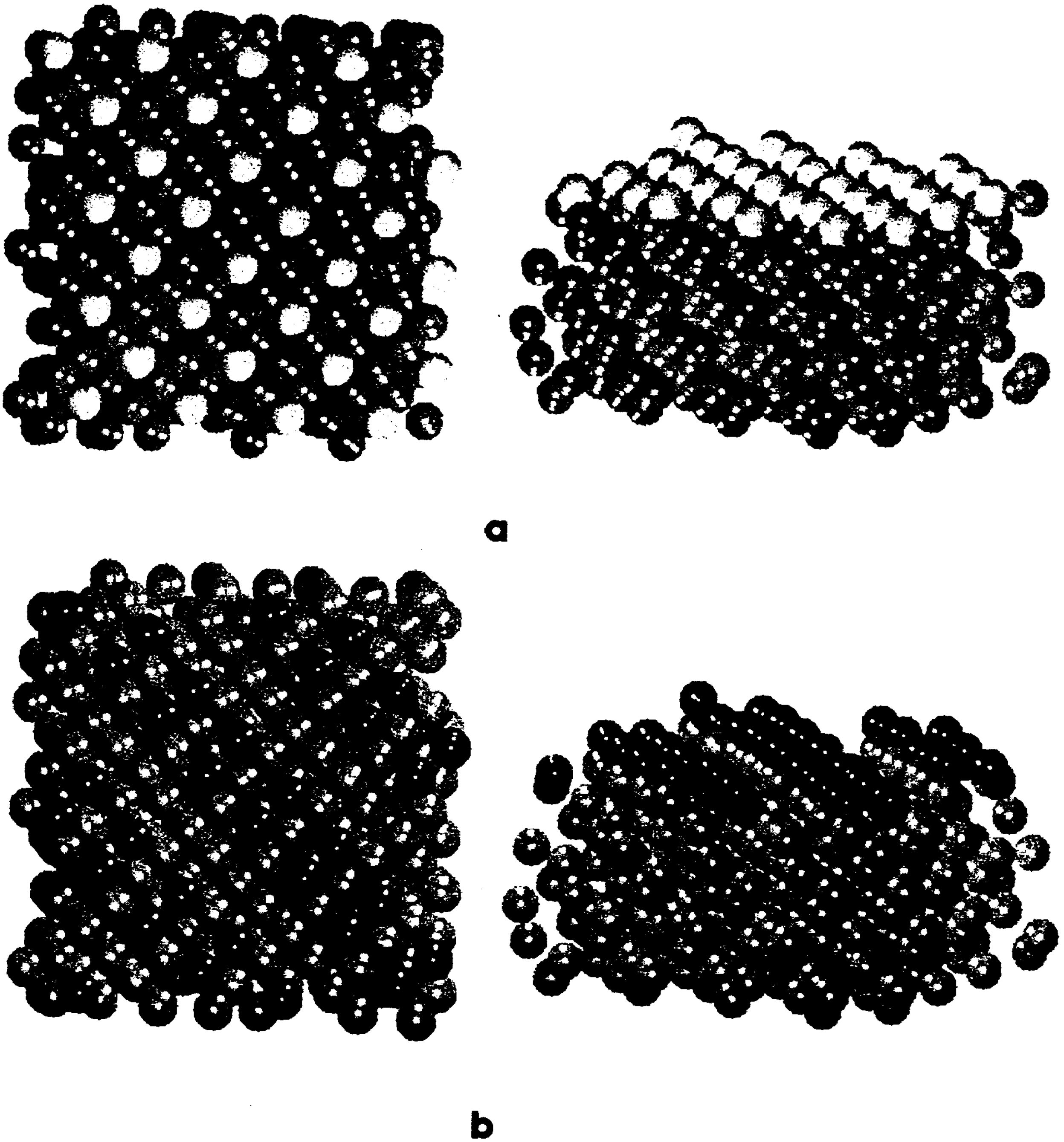

Figure 1. Top and side views of (a) the bulk terminated, and (b) (2 × 1) dimer reconstructed Si{100} surface. Si atoms are colored according to their coordination numbers. Atoms in the bottom most layer and the remaining bulk, where they are 4-fold coordinated, are blue. On the reconstructed surface (b), surface atoms have moved closer to the neighboring atoms and have formed rows of stable (2 × 1)-dimer reconstructions. Dimer atoms with 3-fold coordination are dark blue.

$$E = \sum_i (1/2) \sum_{j \neq i} F_c^{\,ij} [F_R^{\,ij} + B^{ij} F_A^{\,ij}] \qquad (2a)$$

with

$$B^{ij} = -C^{ij} f\Big(\sum_{k \neq i,j} F_c^{\,ik} G(\theta_{ijk})\Big) \qquad (2b)$$

The pair attractive and repulsive interactions in the potential are given by F_A and F_R, respectively, and F_c is a cutoff function that constrains the interaction to be short range. The many-body effects (equivalent for this case to the chemical realism) are included in the summation in eq 2b. Tersoff has fit the parameters (B^{ij}, C^{ij}, and others in $G(\theta_{ijk})$) to bulk properties of Si and Ge.[19] Here we have written the full potential in a compact notation to emphasize that (i) for each pair of atoms i and j the many-body effect comes in through a summation k over all the remaining atoms and (ii) F_c, the cutoff function which sets the limit of short range interactions, is the coefficient of both the pair as well as the many-body interactions in the potential. The main time-consuming part of a molecular dynamics code involving realistic potentials is the computation of forces on hundreds of atoms at millions of time-steps. For short range interactions, however, the concept of a neighbor list,[20] which is a dynamic bookkeeping of the number of atoms within the cutoff distance of each atom in the system, is used. Instead of the sums in eq 2 running over hundreds of atoms, we keep track of the atoms that are close to atom i. During a chemical reaction event, the neighbors of each atom change relatively

---

(20) Abraham, F. F. *Adv. Phys.* **1986**, *35*, 1–111.

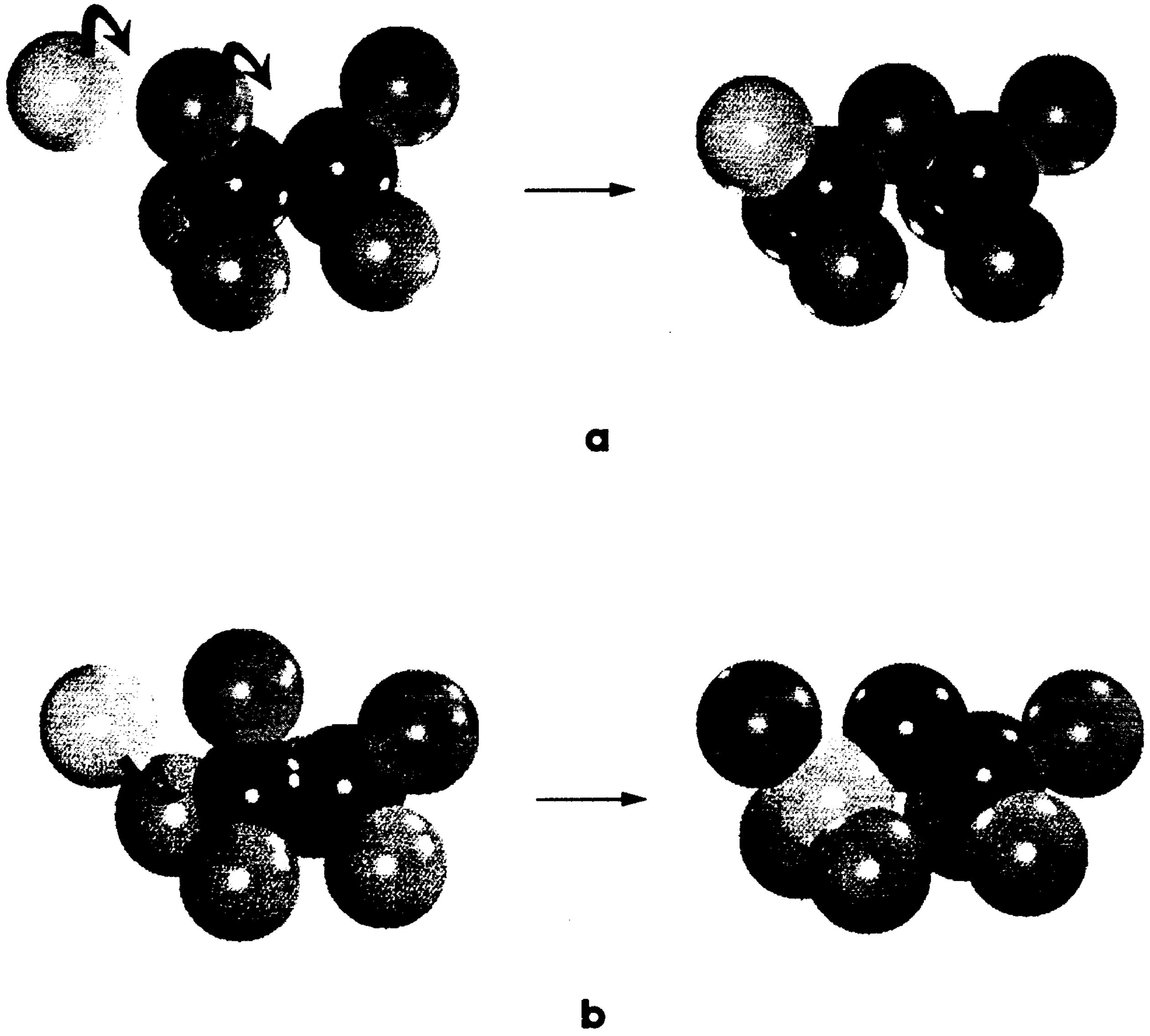

Figure 2. Diffusing adatom motion induced mechanisms of dimer openings. Only a subset of atoms are shown. (a) The inner layer surface Si atoms with 4-fold coordination are blue, the original surface dimer Si atoms with 3-fold coordination are dark blue. Adatoms on the dangling bonds are red and the diffusing adatom is pink. The curly arrows indicate roughly the positions to which adatoms and dimer atoms move during 0.5–1.0 ns of equilibration. The atom colors do not change so that the origins of each atom can be determined. (b) Same as part a except that the mechanism is that of the formation of a defect.

slowly with time and the neighbor list must be updated at regular intervals.

Our molecular dynamics simulation consists of maintaining 10 layers of silicon with 32 atoms/layer. The atoms in the bottommost layer were anchored in position with the atoms in the next four layers forming a stochastic region. The atoms in the top five layers and all the deposited atoms are considered "real atoms" and move only under the influence of the interaction potential. The atoms in the stochastic region experience the forces due to the interaction potential and a frictional force. The magnitude of the friction constant is proportional to the temperature of the system.[21] As the temperature of the system rises (falls) due to physical or chemical interaction between the substrate and the deposited atoms, the magnitude of the frictional forces on the atoms in the stochastic region is increased (decreased) proportionally to damp high (low) temperature oscillations of these atoms. The stochastic region, therefore, facilitates the flow of kinetic energy into and out of the system and maintains a constant temperature. The separation of the full system into an interaction region (top five layers) and a stochastic region (bottom four layers) makes dissipation of excess energy into the stochastic region rather slow, but the dynamics in the interaction region is more accurate and is a better representative of the true dynamical behavior of the interaction potential. The top surface layer (Figure 1b) initially consists of 16 dimers, which are arranged in rows. Periodic boundary conditions that simulate an infinite surface were employed along the surface plane. The structure with neatly arranged rows of dimers has been used in previous simulations of epitaxial growth[8-10] and has also been observed in direct STM studies.[11-14] The deposition rate of Si and Ge atoms at 1 atom/2–3 ps (1 ps = 10^{-12} s) is sufficiently slow so as to allow equilibration of the system before the arrival of the next atom. It has been pointed out in an earlier study[22] that if the deposition rate is too fast to allow for complete

---

(21) Berendsen, H. J. C.; Postma, J. P. M.; van Gunsteren, W. F.; Dinola, A.; Haak, J. R. *J. Chem. Phys.* **1984**, *81*, 3684.

(22) Biswas, R.; Grest, G. S.; Soukoulis, C. M. *Phys. Rev. B* **1988**, *38*, 8154.

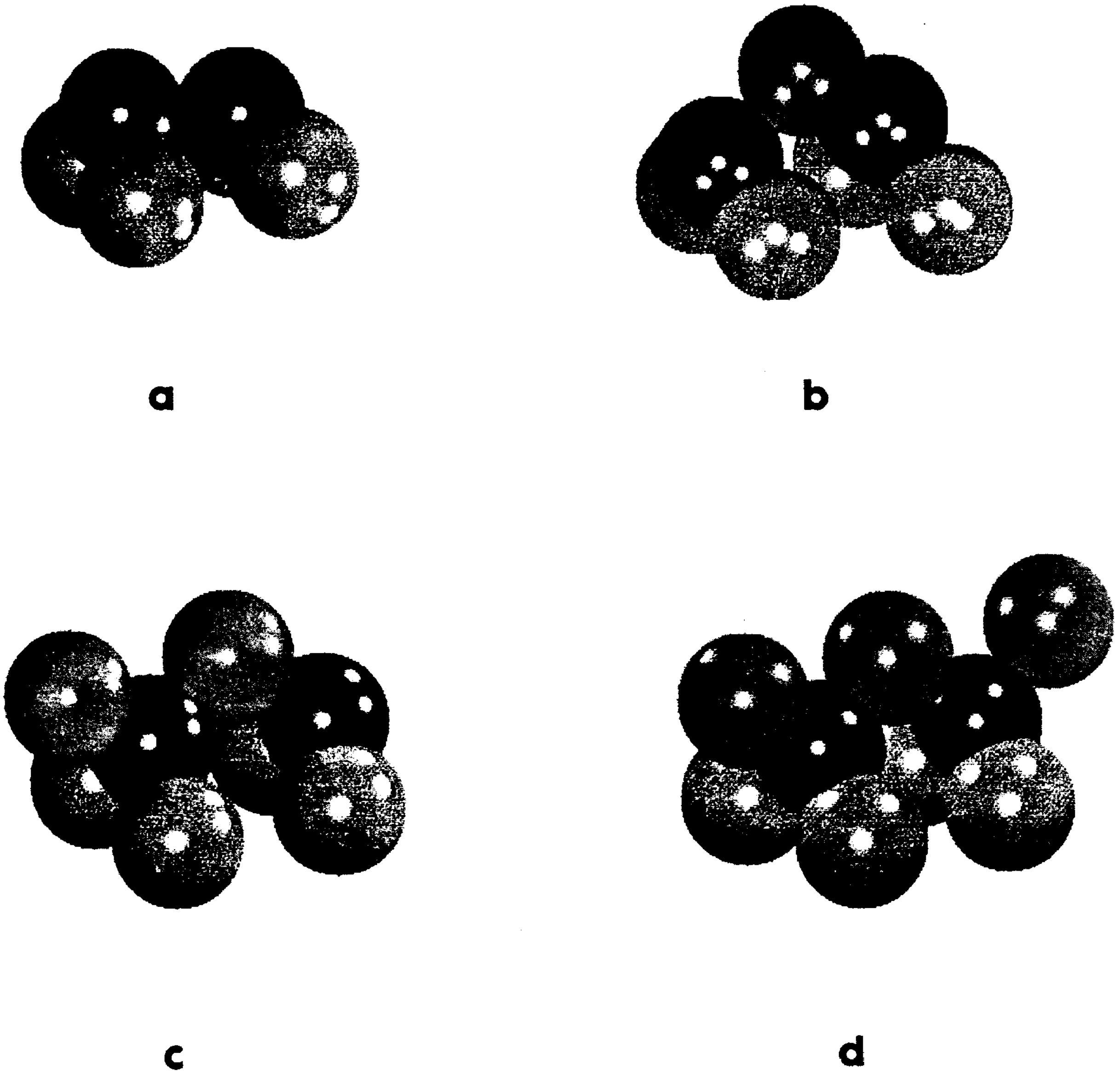

Figure 3. Direct insertion mechanism of dimer opening: (a) Bare surface dimer before deposition. (b) Direct insertion of a gas atom into a dimer. (c) Same as part b except one dangling bond site is occupied. (d) Same as part b except both dangling bond sites are occupied. The coloring is the same as in Figure 2.

dissipation of the kinetic energy from exothermic adsorption reactions, then the excess energy in the interaction region effectively destroys the structure of the interface of the originally reconstructed surface and the layers of the deposited material. The effect of long-time equilibration after the deposition, in that case, is like the simulation of crystallization from a liquid state. After each deposition of 1.5 monolayers of atoms, the full system was equilibrated for 0.5–1 ns. The dynamic behavior of the deposited and the substrate atoms revealed microscopic and macroscopic features of the growing film.

Microscopic Mechanisms of the Initial Stages of the Epitaxial Growth

A comprehensive picture of the initiation of growth of thin epitaxial films on the Si{100}-(2 × 1) reconstructed surface can be partitioned into three stages. First there are the atomic level details of the individual dimer openings (an essential step for the initiation of the epitaxial growth). Second there is an intermediate stage where the initially deposited adatoms begin to resemble the first epitaxial layer. Finally the macroscopic growth modes appear where some systematics of the layer by layer growth process can be established and compared with experimental observations. In the first study of its kind, we present details of the microscopic mechanisms of individual and correlated adatom motion induced collective surface dimer openings. The effect of the latter is to introduce an anisotropy in the epitaxial growth which is directly observable in laboratory experiments such as STM.[11-14] Macroscopic growth modes for depositing a few layers of Si and Ge on the Si{100}-(2 × 1) surface and the comparison of our predictions with other experimental observations will be made in the next section.

Microscopic Mechanisms of Individual Dimer Openings. The microscopic mechanisms of stable dimer openings (those dimers that remain open for the entire duration of simulation) are basically of two types. First is the diffusing adatom induced mechanism, the typical examples of which are shown in Figure 2. The Si and Ge adatoms move as shown by the arrows in Figure 2a during the equilibration period (0.5–1.0 ns). First, both the dangling bonds of an isolated dimer are saturated with two adatoms. A third adatom diffuses over a period of hundreds of picoseconds, to move closer to the dimer, and

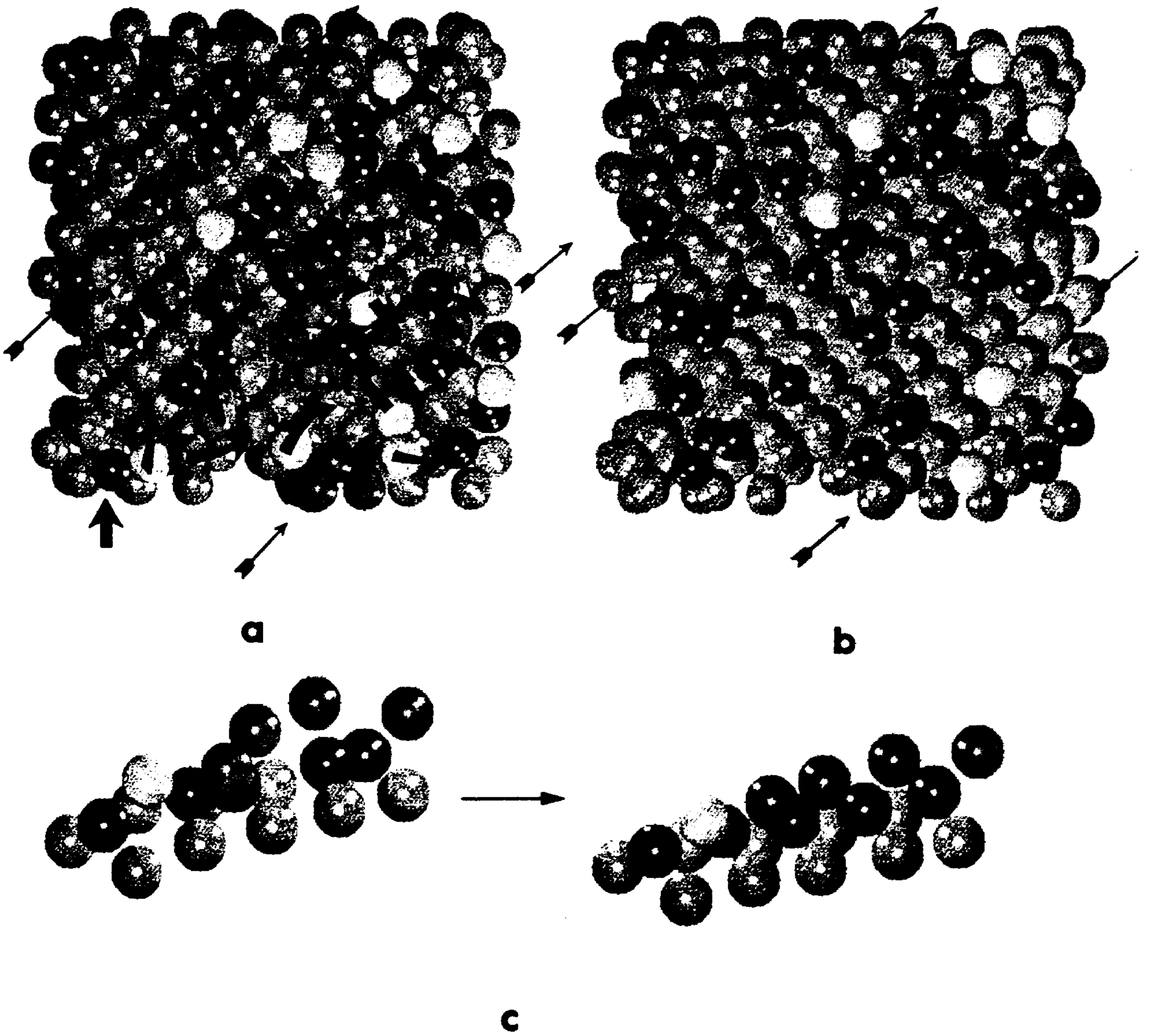

Figure 4. Anisotropic dimer opening mechanism. (a) The original reconstructed surface of Figure 1b after the deposition of 1.5 monolayers of Si atoms at 800 K. The original unopened surface dimer atoms are still dark blue. The subsurface Si atoms, surface atoms where the dimers have opened, and the deposited adatoms with 4-fold coordination are blue. The surface atoms and the adatoms with 3-fold and 2-fold coordination are red and pink, respectively. The curly arrows indicate the directions the adatoms move in the next 0.512 ns. The straight arrows on the side of the crystal are a guide to the periodic boundary conditions and the correlated adatom motion mechanism (see text). (b) The surface and 1.5 monolayers Si adatoms after about 0.512 ns equilibration at 800 K. The atom coloring scheme is same as in part b. The right lower half as well as the part of the upper half, which is connected to the bottom by periodic boundary conditions (straight arrows), has started to show epitaxial growth. The top right corner has three unopened dimer and an amorphous region above it. (c) Anisotropic dimer opening mechanism, which started in the lower left corner of part a, in isolation. The arrow in the lower left corner of part a indicates the sequence of motion shown in isolation in part c. The figure shows position of dimer atoms and adatoms before (c) and after (d) correlated adatom motion induced openings.

pushes the adatom on the dangling bond into the epitaxial position. The diffusing adatom itself then occupies the vacant dangling bond of the open dimer. The three adatoms finally occupy the epitaxial positions, whereas the dimer atoms have relaxed back to their bulk positions. Another observed mechanism of the diffusing adatom induced dimer opening is shown in Figure 2b. Instead of pushing the adatom on the dangling bond into the epitaxial position, in this case, the diffusing adatom can move underneath the adatom on the dangling bond and push the dimer atom into the epitaxial position. In this case, the diffusing adatom has moved into the top substrate layer whereas the substrate dimer atom has moved up into the epitaxial layer. The end products in the homoepitaxy of Si/Si or Ge/Ge, as shown in parts a and b of Figure 2 are the same. However, in case of the heteroepitaxy of Ge/Si this will cause the formation of a defect at the interface. This defect is formed during the growth event and is not due to interlayer diffusion during an annealing process. In other words, the final configuration in Figure 2a does not convert to the one in Figure 2b and vice versa during annealing.

In the second distinct mechanism of surface dimer openings, the atoms in a surface dimer are constantly in motion about their equilibrium positions with amplitudes determined by the temperature of the substrate. During these motions the surface dimers would spontaneously open sufficiently far from their equilibrium separation so that an incoming adatom is directly inserted into the available epitaxial position and thus stabilizes the opening. As shown in Figure 3, we found that the direct insertion of the adatom into epitaxial positions can occur on a bare dimer, on a dimer with one dangling bond occupied, and also on a dimer with both of its dangling bonds occupied.

Most of such direct insertion mechanisms occurred during the deposition process, i.e., the surface was relatively clean. The number of such occurrences increased with an increase in the temperature of the substrate. Above room temperature (800–1200 K) and during the equilibration period, it was also noticed that occasionally a spontaneously opened bare dimer on a relatively clean surface would remain open for hundreds of picoseconds until being stabilized by the direct insertion mechanism. At higher temperatures (1200 K as compared to 800 K for Tersoff's Si potential) the direct insertion mechanism was the primary reaction mechanism of surface unreconstructions.

In a similar study[8] of the epitaxial growth using a different interaction potential,[23] the diffusing adatom motion mechanism was the main mechanism of stable dimer openings, but the total number of such observed openings during a 0.5 ns equilibration period was comparatively smaller. Therefore, no macroscopic growth of several monolayers was achieved. In the same study some unstable open dimers due to the insertion of two or more adatoms were also observed. These unstable openings and the resultant structures are not observed in the present simulations. We believe that the higher surface stabilization energy of that potential[8] (2.1 eV/dimer) vs (1.45 eV/dimer) for the Tersoff's potential[19] and the shorter equilibration times of that simulation may have caused the observed differences.

Correlated Adatom Motion Induced Anisotropic Spread of Surface Unreconstructions. We now discuss a *novel* anisotropic spread of surface dimer openings in the direction perpendicular to the dimer rows on the original reconstructed surface.[9] This correlated reaction mechanism dramatically enhances the crystal growth process in one direction as confirmed in recent STM studies.[11-14] Details of this correlated adatom motion induced dimer openings are exhibited in Figure 4a,b. In Figure 4a we show the result of depositing 1.5 monolayers of Si atoms on the surface over a time span of 144 ps. About half of the deposited atoms are on the dangling bond sites. The remaining atoms either are at the level of the second deposited layer or form a random overlayer at the level of first deposited layer. The observation that the deposited atoms first attach to dangling bond sites is identical with a previous study[8] that used a different many-body interaction potential.[23] During the deposition process four of the original surface dimers were found to open. Two of the openings were due to the direct insertion mechanism, Figure 3, and the remaining two were due a diffusing adatom induced mechanism Figure 2. In one of these later cases the adatom actually replaced one of the original dimer atoms (Figure 2b).

The curly arrows in Figure 4a indicate the atomic motion that occurs in the next 512 ps of equilibration at 800 K. At this later time the majority of the original surface dimers have opened (Figure 4b). One sequence of relevant motion starts in the direction of the straight arrow at the bottom of crystal shown in Figure 4a. The adatoms move in the direction of the arrows with dimers opening along the way. Due to the presence of periodic boundary conditions the continuation of the motion (follow the straight arrows) proceeds to the upper left part of Figure 4a. This string of open dimers is perpendicular to the original dimer rows (Figure 1b). The correlated motion of adatoms inducing a dimer opening does not appear to be dependent on the periodic boundary conditions. This can be seen in another set of correlated motions, which initiate at the lower left corner of the surface in Figure 4a and is terminated only when an amorphous region is encountered as is shown in the upper right corner of the figure. An isolated picture of this later case is shown in Figure 4c. Initially the adatoms are bonded to dimer atoms at the dangling bond positions. This mechanism is a repetition of the mechanism shown in Figure 2a. A cooperative or correlated motion occurs in which the atoms move perpendicularly to the original dimer rows. The final configuration is shown on the right side of the picture. All the adatoms are in the epitaxial positions and all the original surface dimers are open. We note that some correlated motion mechanisms were observed in the overlayer structures also, and they too were terminatged only when they encountered an amorphous region.

Figure 5. Section of STM image taken during MBE (from ref 9 and supplied by R. Hamers). The figure shows a single atom high step going from the upper left corner to the lower right corner. The original dimer rows on the lower step terrace (upper right corner) are parallel to the step edge. The dimer rows on the upper terrace (lower left corner) are perpendicular to the step edge. Only a few tenths of a monolayer of Si atoms have been adsorbed on the surface. The lighter the atoms the higher they are.

Recent experiments that examine the MBE growth on Si{100} using the STM[11-14] have observed surface structures that are indicative of our mechanism of anisotropic growth. Shown in Figure 5 is a portion of one of the scanning tunneling micrographs of a Si{100} surface[9,11] (see figure caption for a description of the surface). The first epitaxial layer is partially present. One of the most striking features in this figure is the long single rows of dimers on both the lower and upper terraces. Based on our simulations these single dimer rows can readily occur because of the correlated adatom motion that leads to dimers opening in a direction perpendicular to the original rows.

Macroscopic Growth Modes of Si and Ge Epitaxial Films on Si{100}-(2 × 1) Surface

We have observed two distinct layer-by-layer growth modes of macroscopic Si and Ge epitaxial films. The temperature of the substrate is the main operative parameter

---

[23] Brenner, D. W.; Garrison, B. J. *Phys. Rev. B* **1986**, *34*, 1304.

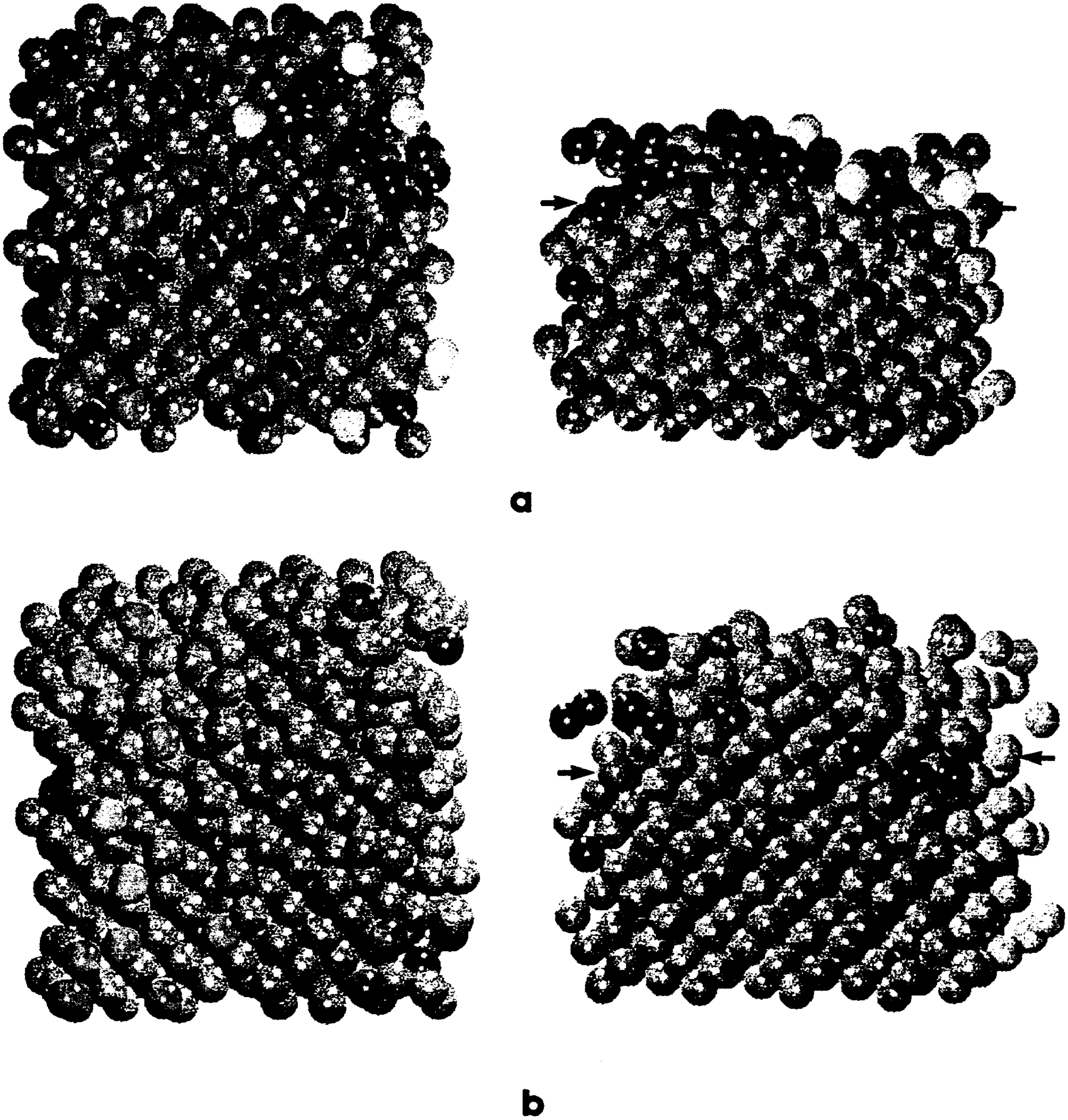

Figure 6. Si/Si{100} at 800 K. (a) The top and side views of the original reconstructed surface after the deposition and equilibration of 1.5 monolayers of Si atoms. The total time in the simulation was 1.1 ns (i.e. another 0.5 ns beyond the configuration shown in Figure 4b). The coloring of atoms is the same as that of Figure 4. The lower right half and top left half of the surface show good epitaxial growth. The upper right corner has unopened dimers and the amorphous growth. The top most atoms in the good epitaxial growth region have started to form random dimer reconstructions. (b) Same as part a except the Si{100} surface is shown after the deposition and equilibration of 4.5 monolayers of Si atoms. The total time in the simulation was 3.4 ns. Persistence of unopened dimers and the amorphous growth throughout the vertical thickness of the interface is apparent in the upper right corner. The lower right half and upper left half of the surface show up to a 4 monolayer thick epitaxial film. In the lower right corner, the atoms of a previously opened dimer on the original surface have closed back again to form the dimer reconstruction.

for the observations of these two distinct modes. In one case, when the substrate temperature is close to the epitaxial temperature,[15] the growth mode is such that the characteristics of the film do not change as more and more layers are deposited and equilibrated. This means that in this case the initially deposited amorphous region remains amorphous throughout the thickness of the interface. In the second mode, reconstructions and unreconstruction can occur in the buried regions of the interface, i.e. the film has tendency to change the growth qualities of its inner layers during long time (nanosecond durations) equilibrations. The temperature of the substrate in the second mode is above the epitaxial temperatures.[15,24] Now we discuss the examples for these two observed modes. For the sake of completeness in the first case we consider the growth of Si/Si{100} at 800 K[9] and in the second of Ge/Si{100} at 1200 K.[10] The primary difference, however, is the temperature. We note that the simulation temperatures of 800 K for Si/Si{100} and 1200 K for Ge/Si{100} do not correspond directly to the experimental 800 K and 1200 K temperatures, respectively.

---

(24) Gossmann, H.-J.; Feldman, L. C.; Gibson, W. M. *Phys. Rev. Lett.* **1984**, *53*, 294.

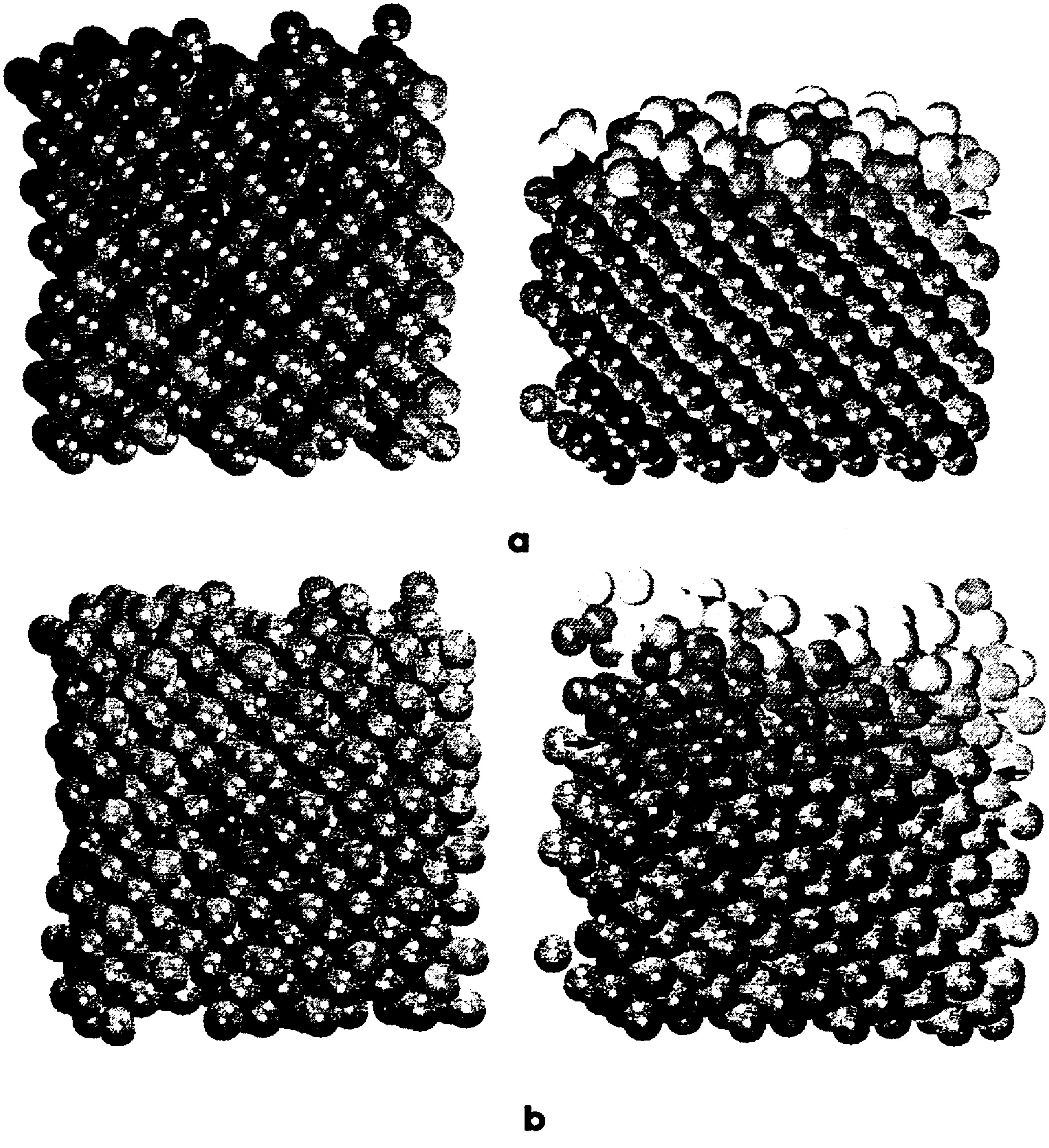

Figure 7. Ge/Si{100} at 1200 K. (a) The side and the cross-sectional view of the Ge/Si interface after the deposition and equilibration of 1.5 monolayers of Ge atoms at 1200 K for about 1.3 ns. All bulk Si atoms (4-fold coordinated) are blue, and Ge atoms are orange. Ge atoms in the interface layer, which show (2 × 2) dimer reconstruction in the upper left corner are red. The 3-fold coordinated Ge atoms are tan and the 2-fold coordinated Ge atoms are yellow. All the dimers on the original Si surface are open and the first epitaxial Ge layer is complete. One interchange of the Si surface atom and the epitaxial Ge atom, which occurred during the deposition (Figure 2b) process, is seen on the lower right corner. (b) Ge/Si interface after the deposition and equilibration of 4.5 monolayers of Ge atoms. The oldest Ge atom is about 2.2 ns. The (2 × 2) dimer reconstruction in the Ge epitaxial layer is almost relaxed. Only a single Ge dimer is left on the interface, which by now is buried under 3.5 monolayers of Ge atoms. To show the top views in parts a and b, we have removed 2 monolayers and 3.5 monolayers of Ge atoms, respectively, from the top.

This is because Tersoff's potential,[19] fit to accurately produce bulk elastic properties and surface reconstruction, does not correctly give either the experimental melting or solid to liquid phase transition temperatures.[25] In a constant pressure molecular dynamics simulation of the melting of bulk Si and Ge we determined that an upper limit on the melting temperatures, T_m, of both Si and Ge is about 3200 ± 50 K. These not only are far from the experimental melting temperatures of Si ($T_m = 1683$ K) and Ge ($T_m = 1211$ K)[26] but also do not yield the correct ratio of the temperature dependent energetics of Si vs Ge. Partly, this can be taken care of by assuming a linear relationship between the experimental and the simulation

---

[25] Stillinger, F. H.; Weber, T. A. *Phys. Rev. B* **1985**, *31*, 5162.

[26] Ashcroft, N. W.; Mermin, N. D. *Solid State Physics*; Holt, Rinehart and Winston: New York, 1976; Chapter 23.

melting temperatures and stating the simulation temperatures as a fraction of the melting temperature. This means that the growth of Si/Si{100} occurs at $0.25T_m$ and that of Ge/Si{100} is at $0.38T_m$, where $T_m = 3200 \pm 50$ K is the simulation melting temperature of Si. Replacing T_m in the above by $T_m = 1683$ K, the experimental melting temperature of Si, it is not difficult to see that the simulation temperatures 800 and 1200 K correspond approximately to the experimental values of 420 and 640 K, respectively. The former is therefore slightly below the experimental epitaxial temperature of Si/Si{100},[15] whereas the latter is above the experimental epitaxial temperature of Ge/Si{100}.[24] The point to emphasize in these simulations is not the exact temperature dependence but the relative behavior and the energetics of the processes at two different temperatures.

Epitaxial Growth of Si/Si{100}. In the first example, we discuss growth of a few layers of Si on Si{100} simulated at a substrate temperature of 800 K. The characteristic features of this growth mode can be explained from Figure 6. In Figure 6a, we show the original dimerized Si{100} surface (Figure 1b) after deposition and about 1.3 ns duration equilibration of 1.5 layers of Si adatoms. Except for three unopened dimers in the upper right hand corner of the figure, the rest of the original Si surface is completely unreconstructed. Some of the adatoms at the level of the first and the second deposited layers have started to form new surface dimers, and a formation of the first epitaxial layer has started in the region where dimers of the original reconstructed surface are relaxed back to their original bulk positions. Of note is that the newly formed surface dimers in the first and second epitaxial layers are randomly placed. This is because Tersoff's empirical potential does not predict that the ordered rows of dimers, as in the (2 × 1) reconstruction, have a lower energy than an equivalent number of randomly placed dimers. In Figure 6b, on the same interface we show an epitaxial growth of up to four monolayers of the deposited material. This was achieved by depositing 1.5 layers of Si atoms, equilibrating for about 1 ns, and by repeating the entire procedure once again. The initially deposited atoms, therefore, are present for about 3.4 ns. For clarity, some of the atoms in the fifth and sixth deposited layers are not shown. There are about 0.5 monolayer per layer in the third and fourth deposited layers. In the epitaxial region initiated by dimer openings shown in Figure 6a, the reconstruction stays constantly at the vacuum-solid interface while the next to the last layer is constantly rearranging. This observation is in agreement with results from Rutherford backscattering experiments.[15] Moreover, we also note that the epitaxial growth characteristics of the first deposited layers are continuously passed on to the growth characteristics of the later deposited layers. This means that the domains of good epitaxial growth in the first four deposited layers are roughly in the same area of the original surface in which the dimer atoms had rearranged back to their bulk positions.

Epitaxial Growth of Ge/Si{100}. We have examined next the deposition of Ge on the (2 × 1) dimer reconstructed Si substrate maintained at 1200 K. The insertion of incoming Ge atoms into the epitaxial positions to stabilize a spontaneously opened dimer (Figure 3) is the most important mechanism of surface unreconstruction during the deposition period. Two diffusing adatom induced dimer openings during the equilibrium of the initially deposited 1.5 monolayers are also observed. In Figure 7, we show the dynamic evolution of the first epitaxially deposited Ge layer as the full simulation of the deposition and equilibration of up to 4.5 monolayers of Ge atoms is performed. In Figure 7a the original Si surface and the first epitaxial Ge layer are shown after 1.3 ns has elapsed. One notes that by now all the dimers in the fully reconstructed original Si surface in the beginning of the simulation have opened. However, in the upper left corner of the figure, about one-third of the first Ge epilayer exhibits a (2 × 2) dimer reconstruction. After the deposition and equilibration for 2 ns of an additional 1.5 monolayers of Ge atoms, the first epitaxial Ge layer and the original Si surface have the configurations shown in Figure 7b. At this point in the simulation, the originally reconstructed Si surface is fully unreconstructed and the first Ge epilayer at the Ge/Si interface, which is buried under 3.5 layers of additional Ge atoms, has only one reconstructed dimer remaining. In contrast to the growth of Si/Si{100}, the unreconstruction of the original Si surface and the first Ge epilayer at the Ge/Si interface buried with 3.5 layers of Ge can occur during the nanosecond time scale equilibration period. This means that the growth characteristics of the initially deposited Ge layers will change as the system is equilibrated because the buried reconstruction at the interface has a tendency to heal itself.

Prospects

We have modeled the *microscopic* mechanisms of atomic motion and the *macroscopic* modes of thin film growth in semiconductor systems. This work is significant in that it is the *most complex* chemical reaction system studied in detail to date. The simulation also allows the motion of ~400 atoms to be followed for up to $3^1/_2$ million timesteps—a real tour-de-force. The results from these calculations have offered new insight into the interpretation of experimental data. Studies of this magnitude and realism are only now possible since the advent of supercomputers.

The future of molecular dynamics simulations for studying chemical reactions at surfaces is extremely promising. Computers will only get faster, more powerful, and less expensive. Activity in developing realistic potentials is booming now that it is possible to test their validity with large scale molecular dynamics simulations. We are approaching a point where computer simulations will be performed as a significant guide to experimentalists.

Acknowledgment. We graciously thank the Office of Naval Research, the National Science Foundation, the IBM Program for the Support of the Materials and Processing Sciences, and the Camille and Henry Dreyfus Foundation for financial support. The Pennsylvania State University supplied a generous grant of computer time on an IBM3090-600S/VF for this work. The manuscript was critically read by Professor Nicholas Winograd at The Pennsylvania State University. Dr. R. Hamers at IBM (Yorktown Heights) provided the STM micrograph used in Figure 5.

Registry No. Si, 7440-21-3; Ge, 7440-56-4.